Steel and Composite Structures, *Vol. 34, No. 3 (2020) 347-359*
DOI: https://doi.org/10.12989/scs.2020.34.3.347

Experimental study on axial compressive behavior of welded built-up CFT stub columns made by cold-formed sections with different welding lines

Morteza Naghipour[1a], Ghazaleh Yousofizinsaz[1b] and Mahdi Shariati[*2,3]

[1]Department of Civil, Babol Noshirvani University of Technology, Babol, Iran
[2]Division of Computational Mathematics and Engineering, Institute for Computational Science, Ton Duc Thang University, Ho Chi Minh City 758307, Vietnam
[3]Faculty of Civil Engineering, Ton Duc Thang University, Ho Chi Minh City 758307, Vietnam

(*Received April 13, 2019, Revised October 11, 2019, Accepted November 1, 2019*)

Abstract. The objective of this study is to experimentally scrutinize the axial performance of built-up concrete filled steel tube (CFT) columns composed of steel plates. In this case, the main parameters cross section types, compressive strength of filled concrete, and the effect of welding lines. Welded built-up steel box columns are fabricated by connecting two pieces of cold-formed U-shaped or four pieces of L-shaped thin steel plates with continuous penetration groove welding line located at mid-depth of stub column section. Furthermore, traditional square steel box sections with no welding lines are investigated for the comparison of axial behavior between the generic and build-up cross sections. Accordingly, 20 stub columns with thickness and height of 2 and 300 mm have been manufactured. As a result, welding lines in built-up specimens act as stiffeners because have higher strength and thickness in comparison to the plates. Subsequently, by increasing the welding lines, the load bearing capacity of stub columns has been increased in comparison to the traditional series. Furthermore, for specimens with the same confinement steel tubes and concrete core, increment of B/t ratio has reduced the ductility and axial strength.

Keywords: welded built-up; CFT; cold-formed; welding lines; ductility

1. Introduction

Concrete members are expanded due to Poisson's effect under axial pressure. Therefore, as a brittle material, the general fracture occurs in concrete members when the stress reaches the ultimate limit (Shariat *et al.* 2018). Occurring an earthquake, this fracture might be due to shear failure, bending failure or shear- bending interaction, causing huge losses both in human and economic terms (Zandi *et al.* 2018, Katebi *et al.* 2019). Confining these compression members is considered as a solution to prevent the deformation due to expansion (Chitawadagi *et al.* 2010, Evirgen *et al.* 2014). Concrete also has been cast in different shapes and types where the self-consolidating (Shariati *et al.* 2019c), porous (Toghroli *et al.* 2017, Toghroli *et al.* 2018b, Li *et al.* 2019, Shariati *et al.* 2019a), high strength (Mohammadhassani *et al.* 2014a, Mohammadhassani *et al.* 2014b, Sajedi *et al.* 2019), lightweight and green (Trung *et al.* 2019a) concrete are the most applicable ones. Concrete characteristics divided into two major categories of fresh properties and hardened properties. Fresh properties included the most primitive properties of the concrete such as slump and workability. On the contrary, hardened properties contains a vast critical features as compressive strength, flexural strength, shear strength and corrosion resistance, where different attempts have conducted to enhance these properties as surface protection (Suhatril *et al.* 2019), inclusion of the fibers and cementitious replacement powders (Saberian *et al.* 2018, Davoodnabi *et al.* 2019, Luo *et al.* 2019, Vali *et al.* 2019, Xie *et al.* 2019).

Using fiber reinforced polymer (FRP) plates, ties or spiral stirrup and steel plates are the most common methods for confining concrete members under compression load (Sinaei *et al.* 2011, Luo *et al.* 2019, Xie *et al.* 2019). FRP plates are suddenly broken down under pressure due to their brittleness. As a result, due to the loss of confinement effect for concrete core, the load bearing capacity of the columns will be reduced (Bakis *et al.* 2002, Fam *et al.* 2003, Dai *et al.* 2011, Yan *et al.* 2014, Yan 2016, Yin *et al.* 2016). Unlike FRP plates, steel plates are an elasto-plastic material which provide confinement for the concrete core even after yielding. Steel-concrete composite members have advantages of both materials and is increasing globally because of efficient synergy of them. Among the composite members, concrete filled steel tube (CFT) columns utilize the beneficial properties of materials, which have higher compressive strength, stiffness and larger energy absorption capacity in comparison with RC or hollow steel members. Therefore, using these members is strongly recommended in seismic zones (Arabnejad Khanouki *et al.* 2010, Jalali *et al.* 2012, Yin *et al.* 2016, Khorami *et al.* 2017a, Khorami *et al.* 2017b). Moreover, the concrete core delays the onset of local

*Corresponding author, Ph.D.
E-mail: shariati@tdtu.edu.vn
[a]Professor
E-mail: m.naghi@nit.ac.ir
[b]MS.C.
E-mail: ghyousefi@yahoo.com

ISSN: 1229-9367 (Print), 1598-6233 (Online)

buckling and prevents inward local buckling in steel tube, while the steel tube enhances the strength of the concrete core through confinement (Gupta *et al.* 2014). CFT members have been used in china for many years such as main columns of metro stations in Beijing since 1966 and also in the power plants building since 1970. The newest usage of CFT members in various countries are SEG tower in Shenzhen province, Rongfeng international trade fair in Hangzhou, Canton tower in Guangzhou, Higgo building in Kobe city of japan, Gateway building in the United States, 55 floor Millennium building In Australia and bank of china building in Hong Kong (Han *et al.* 2014). Most CFT members are prismatic, however, diagonal members with a constant cross section can be used for load transferring system in irregular structures. Also, CFT members with tapered cross-section are used for aesthetic or economical purposes (Han *et al.* 2010, Han *et al.* 2014). Cold-formed steel section has also employed for storage uses and industrial applications such as steel racking and upright-beam systems (Shah *et al.* 2015, Shah *et al.* 2016a, Shah *et al.* 2016b, Shariati *et al.* 2018, Chen *et al.* 2019).

Total cost of a structure is always an important factor in construction industry. Nowadays, the use of thin wall tube in CFT columns is progressively becoming popular in construction of buildings to reduce steel amount due to the higher price of steel (Lee *et al.* 2011). In these members, the major part of axial load is tolerated by the confined concrete which is cheaper than steel. One of the main difficulties in use of thin wall tube is premature local buckling, especially in stub columns. Welded built-up steel box section could delay it and increase the strength and ductility of column. On the one hand, time-consuming and costly empirical tests have been as a barricade against the novel and innovative tests, on the other hand, there are appealing methods which could appropriately cover the aforementioned shortcoming. Finite element (FE) and Finite strip methods are the most useful numerical approaches for analytical assessment and prediction methods (Daie *et al.* 2011, Sharafi *et al.* 2018a, Sharafi *et al.* 2018b, Sharafi *et al.* 2018c, Kildashti *et al.* 2019, Mortazavi *et al.* 2020), where some precursor software such as ABAQUS and ANSYS were facilitated this process (Sinaei *et al.* 2012, Shariati *et al.* 2019d, Taheri *et al.* 2019). Furthermore, artificial intelligence techniques have been introduced to structural engineering problems and proved their efficiency on both prediction and optimization of the test results. Even combining different classic numerical methods and optimization techniques have successfully presented reliable results (Chuanhua Xu 2019, Shariati *et al.* 2019b, Shariati *et al.* 2019e, Shariati 2019). These techniques have developed throughout the years and are appealing in order to employ in different structural issues not only for the handy process and even simple calculations compared to the FE method but also for lower time that need to obtain the results (Shariati *et al.* 2014, Ali 2015, Khorramian *et al.* 2015, Khorramian *et al.* 2016, Safa *et al.* 2016, Shahabi *et al.* 2016a, Toghroli *et al.* 2016, Shariati et al. 2020, Sadeghipour Chahnasir *et al.* 2018, Sedghi *et al.* 2018, Toghroli *et al.* 2018a, Mansouri *et al.* 2019, Milovancevic *et al.* 2019, Trung *et al.* 2019b).

2. Literature review

Up to now, several studies have been carried out to identify the performance of welded built-up members (Shariati *et al.* 2010, Shariati *et al.* 2011a, Shariati *et al.* 2011b, Shariati *et al.* 2011c, Shariati *et al.* 2012a, Shariati *et al.* 2012b, Shariati *et al.* 2012c, Shariati *et al.* 2013, Toghroli *et al.* 2014, Shahabi *et al.* 2016a, Shariati *et al.* 2016, Paknahad *et al.* 2018). In a resaerch by (Whittle *et al.* 2009) focusing on axially loaded built-up C-channels, they have assessed the accuracy and conservativeness of the specifications related to the modified slenderness ratio which is mentioned in Specification D1.2 for built-up members. By another research conducted by (Tao *et al.* 2005), the research has conducted a test on concrete-filled steel tubular stub columns with inner or outer welded longitudinal stiffeners under axial compression. The sectional capacity of the composite stub columns has been increased when stiffeners are provided. Generally, the longitudinal stiffeners not only delay the local buckling of the plate panel, but also improve the lateral confinement on the concrete core. The outer stiffened specimens had shown almost the same behavior as the inner stiffened ones, but the stiffeners should have higher flexural rigidities to ensure their effectiveness. The larger D/t ratio is, the larger the rigidity requirement of stiffeners is. A study by (Petrus *et al.* 2006) have investigated an experimental work into the bond strength of a CFST column with tab stiffeners. The found stiffeners have key role in improvement of bond strength at steel–concrete interface. (Lee *et al.* 2011). has experimentally investigated the structural characteristics of square CFT stub columns by using cold formed thin steel plates. They have introduced manufacture method for use of thin walled cold-formed in square concrete filled tubular column. All specimens are fabricated for the test with variables of steel tube type, width–thickness ratio and concrete strength to evaluate structural capacities and behavioral characteristics of welded built-up square CFST columns. The results have shown that welded built-up steel tubes are superior to generic steel tubes with the same width in terms of cross-sectional efficiency because total cross section is effective sectional area in the former. An investigation by (Zeghiche 2013) has presented an experimental and finite element study on the load carrying capacity of thin and composite steel–concrete stubs subjected to direct compression. The studied sections are made of two cold formed U shaped steel plates welded to form a steel box or an I-shaped steel section. All failure loads are predicted numerically using Abacus program and Euro-codes EC3 and EC4 for steel and composite stubs, respectively. A comparison of results has been calculated using FEM model, showing good agreement with test results. However, EC3 and EC4 predictions are not conservative. According to the test results, the length and discontinuous welding fillet for empty stubs has a drastic effect on load carrying capacity and failure mode is mainly a premature local buckling mode. Providing rectangular steel stubs with continuous welding on mid-depth improvedthe load carrying capacity for both rectangular empty steel and composite stubs. CFT columns with

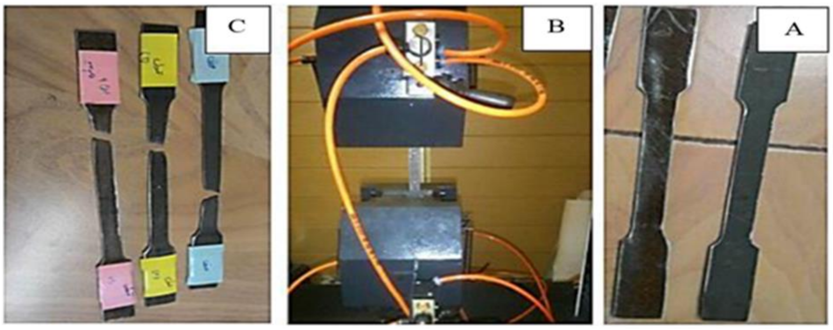

Fig. 1 A: Dumbbell- shaped steel samples before direct tensile test, B: test instrument, C: Samples after direct tensile test

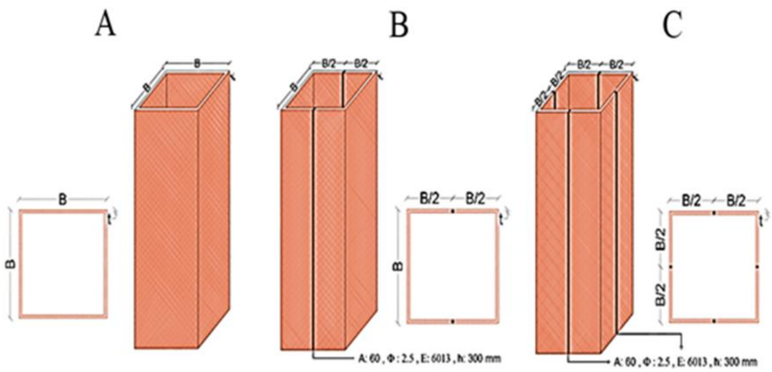

Fig. 2 A: Generic Steel box section, B: Steel box made by connecting two pieces of cold-formed U-shaped steel plates, C: Steel box made by connecting four pieces of cold-formed L-shaped steel plates

continuous welding have a greater lateral stiffness and rupture strength compared to CFT columns with discontinuous welding steel sections. Test results have shown that I-shaped steel stubs has a higher compression load carrying capacity with a lower load decrease rate compared to fabricated rectangular steel stubs with height over 200 mm. I-shaped composite stubs couldn't reach the unconfined strength because the failure mode is by local buckling of steel flange, steel–concrete bond failure and concrete crushing. It is believed that I-shaped composite could reach higher failure loads if they are provided with lateral stiffeners or shear connectors. Using different types of shear connectors while their performance have been conducted recently (Shariati *et al.* 2012a, Shahabi *et al.* 2016a, Shahabi *et al.* 2016b, Tahmasbi *et al.* 2016, Khorramian *et al.* 2017, Hosseinpour *et al.* 2018, Nasrollahi *et al.* 2018, Wei *et al.* 2018, Shariati 2019) could be alternatve options for this purpose.

A resaerch by (Ferhoune *et al.* 2016) has studied the axial bearing capacity of thin welded rectangular steel stubs filled with concrete sand. The findings have shown that the column strengths have been increased when the stubs height is decreased and the sign of local buckling has been developed when the ultimate bearing capacity is reached to the instability of columns.

However, few studies have addressed the influence of different confinement steel tubes with different welding lines (stiffeners) on load capacity of CFT stub columns. To fill this gap, this research has studied the mention configurations in square CFT columns and assessed the load bearing capacity and ductility of them. Also, cold-formed CFT columns with high strength welding lines are used to provide higher thickness and yield stress of welding lines in comparison to steel tubes. Thus, welding lines could be considered as longitudinal stiffeners.

3. Materials

The properties of steel and concrete materials for welded built-up and generic CFT columns are presented in this section.

3.1 Steel

In order to manufacture CFT columns in this research, steel plates and boxes with 2 mm thickness have been used as outer tube. It should be noted that steel boxes with no welding lines (generic) are considered for comparing the axial performance between generic and build-up cross sections made by steel plates. Direct tensile test has been performed according to (ASTM-A370.2017) to obtain the

Table 1 Results of direct tensile strength test for dumbbell-shaped samples obtained from steel box and plate

Tensile strength of steel (MPa)			
Steel box		Steel plate	
Yield stress	Ultimate stress	Yield stress	Ultimate stress
317.4	356.6	361	394.8

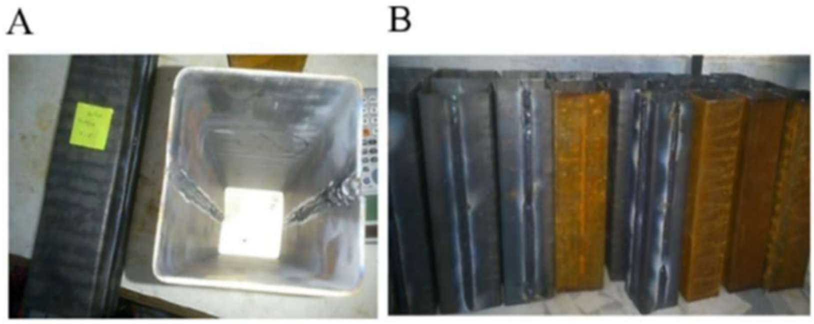

Fig. 3 A: Connection between 2 U-shaped (Dai *et al.* 2011) steel plates with complete penetration groove weld, B: Overall configuration of steel boxes

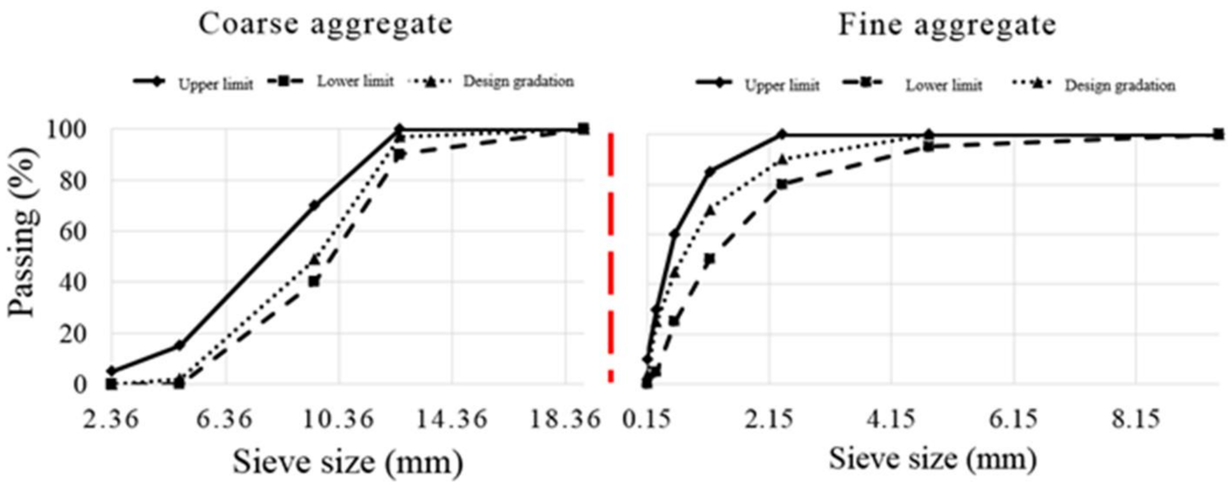

Fig. 4 Design gradation and (ASTM C33M-16.2016) recommendation

mechanical properties of steel plates and boxes. Dumbbell-shaped steel samples obtained from steel plates and boxes before and after direct tensile test and test instrument are shown in Fig. 1.

Table 1 shows the results of tensile strength for dumbbell - shaped specimens obtained from steel plates and boxes. In order to prepare welded built-up specimens, steel boxes have been made by welding 4 (L-shaped) or welding 2 (U-shaped) steel plates. In this study, the height of all specimens is 300 mm to minimize the influence of buckling. Fig. 2 schematically illustrates steel sections which are utilized for the generic and welded built-up CFT columns. In order to manufacture L-shaped and U-shaped steel boxes, steel plates are cut by cutting equipment and then became in the form of L and U- shaped steel plates with iron bending machine. L-shaped and U-shaped steel plates are connected by continuous welding along the edges. Complete penetration groove weld performed by rectifier instruments with A: 60, Ø: 2.5 and E: 6013. The connection between two U- shaped steel plates with complete penetration groove weld and the other steel tubes are demonstrated in Fig. 3.

3.2 Concrete mix proportion

The crushed aggregates and river sand used for manufacturing of core concrete have been provided from the mines in Mazandaran province, Iran. Also, the sieves NO.4 and NO.12 have been used for separating coarse and fine grained aggregates based on (ASTM C1360. 2014). In order to remove dust, aggregates have been washed and dried in an

Table 2 Materials mix proportions for manufacturing concrete

Concrete	Cement	Aggregate (Fine)	Aggregate (Coarse)	Water	Water cement ratio
	Materials content (Kg/m^3)				
20 MPa	307	830	964	215	0.7
30 MPa	391	830	964	215	0.55

Table 3 Compressive strength test results for 28-day cube and equivalent cylindrical concrete

Concrete sample	20 MPa mix design	30 MPa mix design
Compressive strength of 28-day cube concrete (MPa)	27.32	38.58
	27.63	38.03
	27.03	38.97
	26.68	39.11
Compressive strength of 28-day equivalent 150×300 cylindrical concrete	21.85	30.86
	22.10	30.46
	21.62	31.17
	21.34	31.28
Average	21.72	30.94

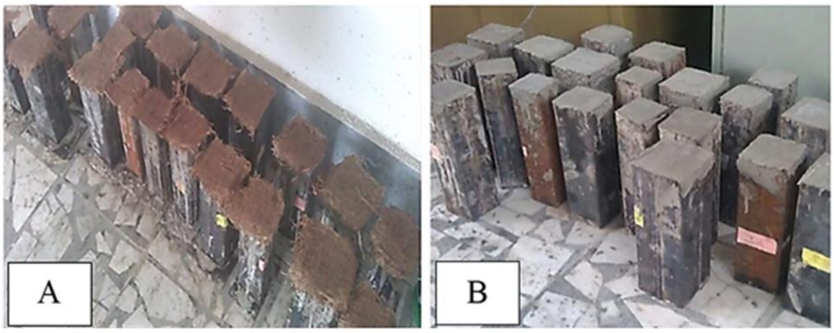

Fig. 5 A: Curing and surface moisture protection by wet sacks, B: CFT columns after 28-day curing

oven. Fig. 4 illustrates the design gradation which is used in this research and (ASTM C33M-16.2016) grading limits. Noticeably, maximum nominal diameter of aggregates is 12.5 mm. Sand equivalent and fineness modulus are determined 0.71 and 3, respectively which are compatible with (ASTM C33M-16.2016) recommended limits. Type II Portland cement has been used for concrete manufacturing.

In this research, concrete with compressive strength of 20 and 30 MPa have been used in CFT columns , also (ACI 211.1.1991) standard is used for manufacturing concrete. According to table 2, material mix proportions with 12.5 mm nominal diameter of aggregates and 80-100 slump are determined according to (ACI 211.1.1991) standard, recommending a 28-day 150×300mm cylindrical concrete samples for controlling the compressive strength. For each mix proportion mentioned in Table 2, four 28-day cube concrete samples have been prepared for compressive strength test by ELE instrument with 200 tons capacity to ensure achieving concretes with desired strength.

The conversion factor equals to 0.8 has been used to convert the compressive strength of cube samples to the cylindrical ones. 28-day compressive strength of cube concrete samples and equivalent cylindrical specimens are presented in Table 3.

Averagely, the manufactured concrete provides the desired compressive strength for CFT columns. All the specimens cast vertically and vibration is provided by shaking table. The curing process and CFT columns at the end of 28 days are shown in Fig. 5.

4. Experimental testing

20 CFT stub columns have been tested in pure axial compression and classified into 3 groups in terms of different

Fig. 6 Overall view of test set-up.

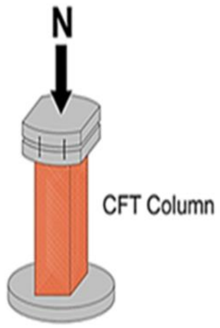

Fig. 7 Compressive axial loading concept

cross sections and concrete strength, which are as follows:
1. Generic CFT columns with no welding lines (BNO specimens).
2. Cold-formed CFT columns with 2 welding lines (U specimens).
3. Cold-formed CFT columns with 4 welding lines (L specimens).

In all specimens, columns have equal height of 300 mm. It should be noted that the generic CFT columns (group 1) are considered as controls to compare with other specimens (2 welding lines and 4 welding lines). Specimens are named by using a naming system including one letter and four numbers. For example, L4-70-2-20 represents a specimen of the welded built-up CFT stub column by connecting four pieces of L-shaped thin steel plates with continuous penetration groove welding line, with 4 welding lines (indicated by the first number, 4). The cross sectional dimension of column is 70 (indicated by the second number, 70).The steel tube thickness is 2mm (indicated by the third number, 2), and the concrete strength is 20Mpa (indicated by the last number, 20). BNO specimens are the CFT columns with no welding lines.

4.1 Test procedure

Loads are applied by a 60 ton UTM at a speed of 3mm/min. The universal machine is equipped with top and bottom jaw. The fixed jaw is placed at the bottom and the movable jaw with free vertical movement is placed at the top. The axial pressure is applied on the top surface of CFT samples by the movable jaw. To ensure that axial pressure load was uniformly applied on the top surface of CFT samples, a special type of movable jaw has been used (Fig. 6). In order to investigate the compressive behavior of CFT samples and buckling type, buckling zones, the occurrence or non-occurrence of rupture in confinement steel or weld zone, the axial pressure load has been applied on the whole cross section of CFT columns (Fig. 7).

As the axial pressure load is applied, the stress-strain curves and the compressive strength for all CFT columns are recorded through a processor connected to test machine. When the results are satisfying, the loading is proceeded until it reached the failure. The results and analysis are subsequently presented.

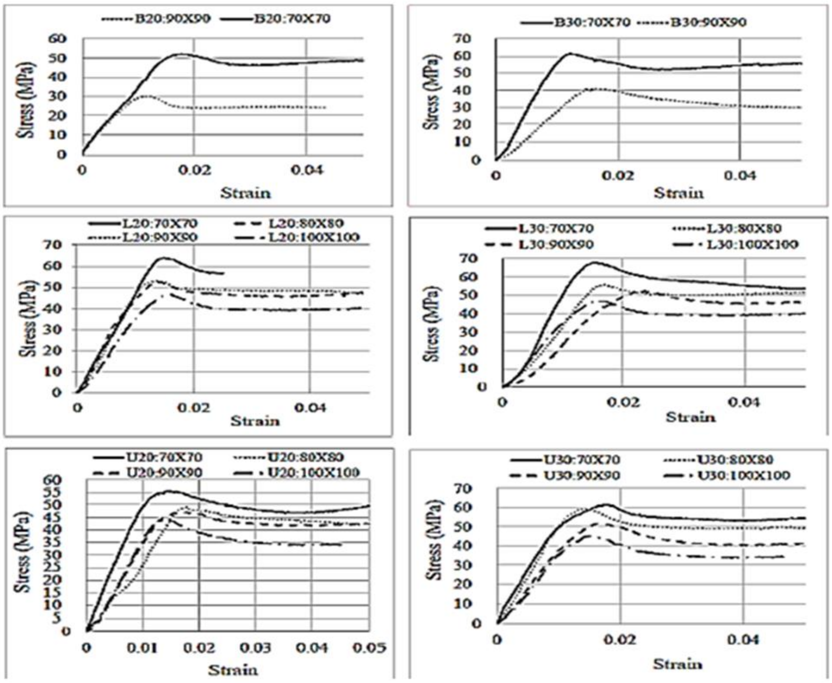

Fig. 8 Stress-strain curves under axial compression for CFT samples

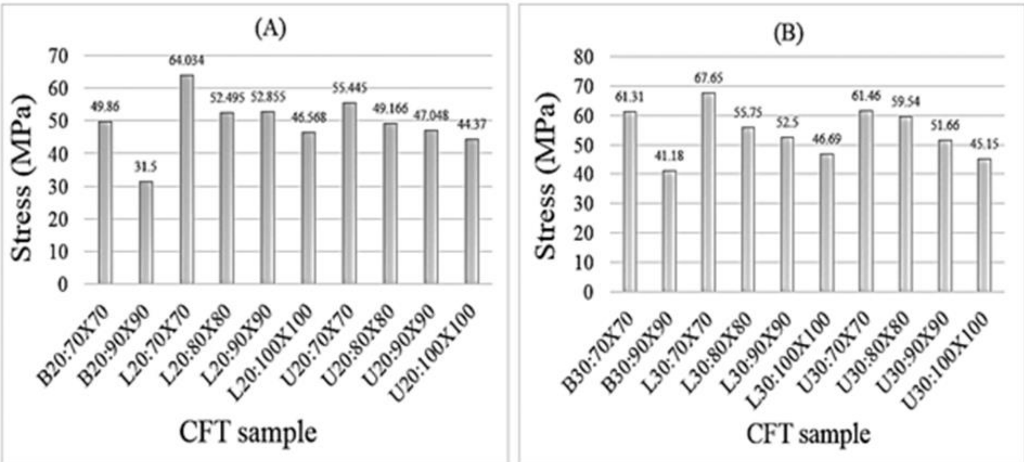

Fig. 9 Ultimate stress of CFT samples, A: 20MPa concrete core, B: 30MPa concrete core

5. Results and discussion

5.1 The axial performance of the CFT stub columns

The stress-strain curves obtained from axial compressive strength test are shown in Fig. 8. All specimens had a smooth descending branch, offering more ductility. It can be seen that for CFT columns with the same confinement steel tubes and concrete, the increment of B/t ratio has reduced the ductility and compressive strength. This is due to the reduction of confinement effect of steel tubes by increasing B/t ratio which is exactly compatible with literature by (Abed *et al.* 2013). The elastic stiffness of CFT columns with 30 MPa concrete is greater than its 20 MPa counterpart. Also, in specimens with different B/t ratios, significant change has been observed in elastic stiffness of CFT columns with concrete strength of 30MPa and with no welding lines due to lack of stiffeners. For easier comparison, the ultimate stress of CFT columns under axial pressure is shown in Fig. 9.

Obviously, the highest load bearing capacity has been obtained from CFT samples with confinement steel tubes which are made by welding 4 (L-shaped) steel plates. While, the reverse is true for CFT columns with no welding lines, it is assumed that for CFT columns with the same dimensions and concrete core, axial load distribution between more welding lines lead to higher ductility and load bearing capacity. This is because welding lines were considered as stiffeners. With the same welding quality, axial pressure load

Fig. 10 Deformation of CFT columns under axial compression

is distributed between (L-shaped) steel plates and concrete core, leading to more ductility and load bearing capacity compared to the load distribution between 2 (U- shaped) steel plates and concrete core.

It is evident that for the same B/t ratios and steel tubes, increasing concrete strength could obtain higher load bearing capacity which is exactly compatible with previous studies about the delay of buckling as the main reasons for this subject (Lee *et al.* 2011). In steel tubes with constant B/t ratios, the effect of welding lines is more effective than concrete strength. The load bearing capacity of B70×70 having concrete strength of 30 MPa is increased by 22.96% when compared with its 20MPa counterpart. This increment in load bearing capacity in case of 4 L-shaped steel plates has reached to a maximum of 28.42% compared to the B70×70 with 20MPa concrete strength.

This is true for all CFT samples in this research. Also, concrete strength has more positive effect on load bearing capacity of CFT samples compared to B/t ratio. In CFT columns made by welding 2 U-shaped steel plates as confinement tubes and 20 MPa concrete strength, the load bearing capacity of 90×90 CFT samples is decreased 4.3% in comparison to the 80×80 samples. While, for 80×80 CFT columns with 2 welding connections, using 20MPa concrete has decreased the load bearing capacity up to 27.09% compared to the 30MPa concrete. This is true for all CFT samples in this research according to Fig. 9. Probably, in CFT columns with greater cross section, further expansion of concrete under axial pressure caused by Poisson's effect leads to negative effects of B/t ratios on load bearing capacity. The final failure modes of CFT columns are presented in Fig. 10. Accordingly, only outward buckling is occurred in CFT samples, approving the beneficial properties of using both concrete and steel in composite members. Inward bugles are prevented by concrete in CFT columns.

Despite high ductility and load bearing capacity, the rupture in CFT samples welded along 4 edges is in weld zone at ultimate stress, while, no rupture has been observed in weld zone at ultimate stress in CFT columns welded along 2 edges. In specimens with similar welding lines, the number of bugles distributed along the height of columns is decreased by increasing the compressive strength of concrete and B/t ratio. Also, the effect of B/t ratios on load bearing capacity of CFT columns with 2 or 4 welding lines is less significant than the columns with no welding connections, due to the welding lines which were used as stiffeners. Regarding the load bearing capacity of B90×90, the concrete strength of 20 MPa is decreased by 36.8% and compared to B70×70. While, for CFT columns with 4 and 2 welding lines, the load bearing capacity is decreased 17.4% and 15.455%, respectively.

5.2 Ductility index

In this study, in order to define the ductility index, displacement method has been used which is defined as the ratio between the displacement corresponding to 85% of maximum load (in the descending branch) and the displacement of the maximum load.

$$DI = \frac{d0.85N\max}{dN\max} \tag{1}$$

CFT columns with 4 stiffeners have presented the highest ductility varying from 1.67 to 1.76 and CFT columns with no welding lines presented the lowest (1.49 to 1.55). Based on Table 4,concrete strength have not significantly influenced the ductility of CFT specimens, though a very slight drop has been observed with the increasing of B/t ratio and concrete strength, while, the effect of welding lines on ductility is greater than concrete strength and B/ t ratio.

Also, CFT columns with 4 welding lines shows up more ductile behavior compared to columns with 2 welding lines

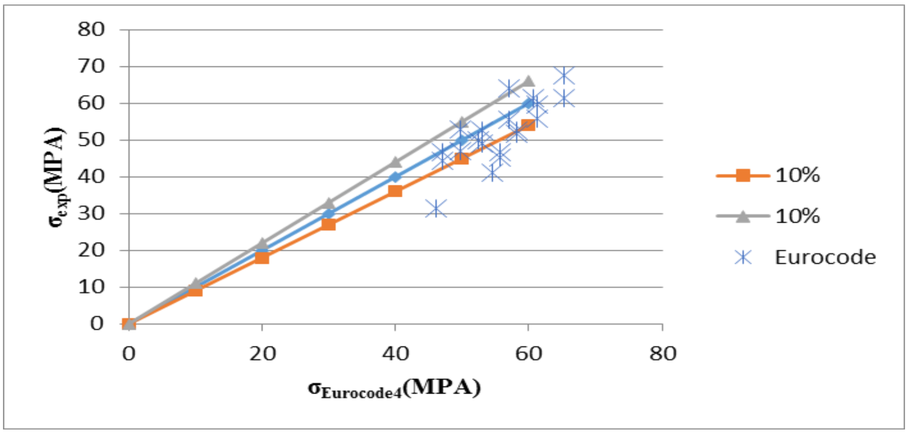

Fig. 11 Comparison between experimental ultimate load and Euro code 4

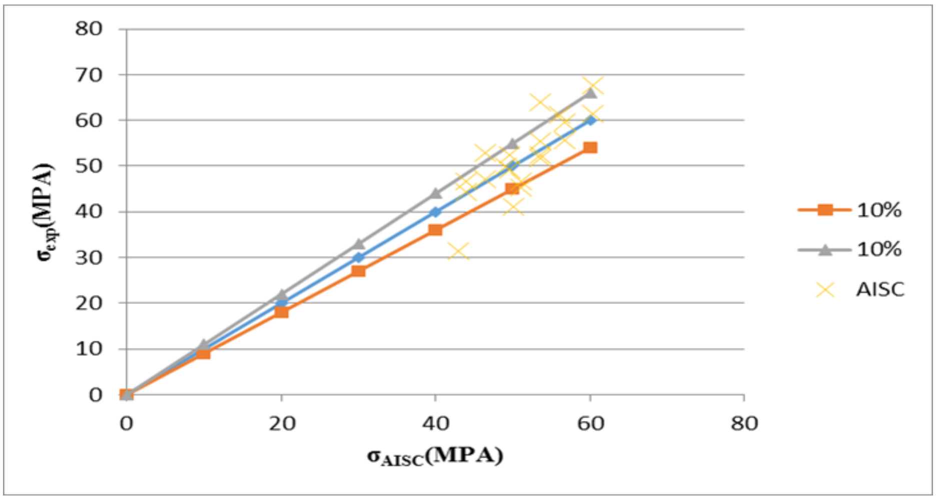

Fig. 12 Comparison between experimental ultimate load and AISC specifications

and columns with 2 welding lines has higher ductility compared to specimens with no welding lines.

6. Comparison with Eurocode 4 and AISC specifications

The design compressive strength N_{AISC} for axially loaded CFST columns can be determined for the flexural buckling limit state based on the member slenderness as follows (AISC.2010)

$$NAISC = \begin{cases} Pn = Pno(0.658\ Pno/\ Pe, & Pno\ /\ Pe\ \leq 2.25 \\ 0.877\ Pe & Pno\ /\ Pe \geq 2.2 \end{cases} \quad (2)$$

Pno is the nominal axial strength of CFST specimens and can be determined by equation 3. where c is 0.85 for rectangular CFST sections

$$Pno = A_S f_y + C\, A_C f_c \quad (3)$$

Pe is the elastic critical buckling load that can be calculated by using Euler's formula shown in Equation 4

$$Pe = \pi^2\, EI_{eff}/\ Lc \quad (4)$$

EIeff is the effective stiffness of CFST section and can be determined by the following equation

$$EI_{eff} = E_s\, I_s + c_1\ \ E_C\, I_C \quad (5)$$

where c_1 accounts for the effective rigidity of filled composite compression member, and is calculated as follows

$$C_1 = 0.25 + 3\ (A_s + A_{sr}/\ A_g) \quad (6)$$

The strength of rectangular CFST stub columns (Nu) in (Eurocode 4.2004) can be expressed as

$$N_u = A_S f_y + A_C f'_c \quad (7)$$

The maximum loads obtained from the experiments and those obtained from Eurocode 4 and AISC specification are shown in Figs. 11 and 12. These values have been presented in Table 4. N_{Exp}/N_{AISC} ratios are inside the safety margin of 10%. And in most cases are on the safe side ($N_{Exp}/N_{AISC} \geq$

Table 4 Test properties and results

No	Name	Geometrical properties (mm) (B)	(t)	L	f'_c	Nexp/NEC4	Nexp/AISC	Nexp/Ncal	DI
1	BNO-70-2-20	70	2	300	21.7	0.95	1.01	0.9	1.55
2	BNO-70-2-30	70	2	300	30.94	1.01	1.09	0.92	1.52
3	BNO-90-2-20	90	2	300	21.7	0.68	0.73	0.89	1.51
4	BNO-90-2-30	90	2	300	30.94	0.75	0.82	0. 9	1.49
5	L4-70-2-20	70	2	300	21.7	1.12	1.19	1.09	1.76
6	L4-70-2-30	70	2	300	30.94	1.03	1.11	0.98	1.72
7	L4-80-2-20	80	2	300	21.7	0.99	1.05	0.97	1.74
8	L4-80-2-30	80	2	300	30.94	0.9	0.98	0.94	1.71
9	L4-90-2-20	90	2	300	21.7	1.06	1.13	1.05	1.72
10	L4-90-2-30	90	2	300	30.94	0.9	0.97	0.96	1.7
11	L4-100-2-20	100	2	300	21.7	0.98	1.06	0.99	1.69
12	L4-100-2-30	100	2	300	30.94	0.83	0.91	0.95	1.67
13	U2-70-2-20	70	2	300	21.7	0.97	1.03	0.94	1.65
14	U2-70-2-30	70	2	300	30.94	0.94	1.01	0.93	1.62
15	U2-80-2-20	80	2	300	21.7	0.92	0.99	0.93	1.64
16	U2-80-2-30	80	2	300	30.94	0.97	1.05	0.92	1.6
17	U2-90-2-20	90	2	300	21.7	0.94	1.01	0.94	1.62
18	U2-90-2-30	90	2	300	30.94	0.88	0.96	0.9	1.59
19	U2-100-2-20	100	2	300	21.7	0.94	1.01	0.94	1.6
20	U2-100-2-30	100	2	300	30.94	0.81	0.88	0.9	1.55

1). While, (N_{EXP}/N_{EC4}) ratios are on the unsafe side ($N_{EXP}/N_{EC4} \leq 1$), though N_{EXP}/N_{EC4} is inside the safety margin of 10%.

5. Conclusions

The main goal of this study is to investigate the axial compressive behavior of CFT columns which is manufactured by steel boxes welded steel plates as confinement tubes. A 28-day concrete with 20 and 30 MPa strength are casted in steel tubes as concrete core. All CFT columns have 300 mm height and the thickness of steel tubes is fixed to 2 mm. Based on the obtained results, the following conclusions could be drawn:

- In CFT columns with the same B/t ratios, by increasing the welding lines, the load bearing capacity of columns is increased compared to the BNO series and this average amount for U2 and L4 series are about 21% and 32.5%, respectively. Welding lines in U2 and L4 series are considered as stiffeners, due to the fact that the welding lines have higher strength and thickness in comparison to steel plates and thus delayed an out ward buckling in CFT columns.
- The load bearing capacity of columns with concrete strength of 30 MPa is increased compared to its 20MPa counterpart, which is more significant in BNO series than the other two series.
- In specimens with similar concrete strength, reducing B/t ratios has increased the load bearing capacity of columns and this is more noticeable in CFT columns with higher concrete strength.
- In steel tubes with constant B/t ratios, the effect of welding lines is more effective than concrete strength and concrete strength has more positive effect on load bearing capacity of CFT samples compared to B/t ratio. Probably, in CFT stub columns with greater cross section, further expansion of concrete under axial pressure is caused by Poisson's effect led to negative effects of B/t ratios on load bearing capacity.
- It was observed that the effect of B/t ratios on load bearing capacity of CFT columns with 2 or 4 welding lines is less significant than the columns with no welding connections, due to the welding lines used as stiffeners.
- The elastic stiffness of CFT columns with 30 MPA concrete is greater than its 20 MPA counterpart. Also, in specimens with different B/t ratios, more significant change is observed in elastic stiffness of CFT columns with concrete strength of 30MPA and with no welding lines due to lack of stiffeners.
- The ductility of CFT columns with more welding lines is greater and increased as B/t ratios is decreased. CFT columns with 4 welding lines have the highest ductility. On the other hand, CFT columns with no welding lines have the lowest ductility index due to lack of stiffeners.

Acknowledgements

The research presented in this paper was supported by Babol Noshirvani University of Technology (Award No: BNUT934140052). The support is gratefully acknowledged.

References

Abed, F., *et al.* (2013), "Experimental and numerical investigations of the compressive behavior of concrete filled steel tubes (CFSTs)", *J. Constr. Steel Res.*, **80**, 429-439. https://doi.org/10.1016/j.jcsr.2012.10.005.

Arabnejad Khanouki, M., *et al*. (2010), "Investigation of seismic behaviour of composite structures with concrete filled square steel tubular (CFSST) column by push-over and time-history analyses", *Proceedings of the 4th International Conference on Steel & Composite Structures*.

Bakis, C.E., *et al*. (2002), "Fiber-reinforced polymer composites for construction—State-of-the-art review", *J. Compos. Constr*., **6**(2), 73-87. https://doi.org/10.1061/(ASCE)1090-0268(2002)6:2(73).

Chen, C., *et al.* (2019), "Behavior of steel storage pallet racking connection-A review", *Steel Compos. Struct.*, **30**(5), 457-469. https://doi.org/10.12989/scs.2019.30.5.457.

Chitawadagi, M.V., *et al.* (2010), "Axial strength of circular concrete-filled steel tube columns—DOE approach", *J. Constr. Steel Res.*, **66**(10), 1248-1260. https://doi.org/10.1016/j.jcsr.2010.04.006.

Dai, J.G., *et al*. (2011), "Behavior and modeling of concrete confined with FRP composites of large deformability", *J. Compos. Constr*., **15**(6), 963-973. https://doi.org/10.1061/(ASCE)CC.1943-5614.0000230.

Daie, M., *et al.* (2011), "A new finite element investigation on pre-bent steel strips as damper for vibration control", *Int. J. Phys. Sci*., **6**(36), 8044-8050. DOI: 10.5897/IJPS11.1585.

Davoodnabi, S.M., *et al.* (2019), "Behavior of steel-concrete composite beam using angle shear connectors at fire condition", *Steel Compos. Struct.*, **30**(2), 141-147. https://doi.org/10.12989/scs.2019.30.2.141.

Evirgen, B., *et al.* (2014), "Structural behavior of concrete filled steel tubular sections (CFT/CFSt) under axial compression", *Thin-Wall. Struct*., **80**, 46-56. https://doi.org/10.1016/j.tws.2014.02.022.

Fam, A., *et al.* (2003), "Precast piles for Route 40 bridge in Virginia using concrete filled FRP tubes", *PCI J.*, **48**(3), 32-45.

Ferhoune, N., *et al.* (2016), "Behavior of hollow thin welded tubes filled with sand slag concrete", *Adv. Mater. Sci. Eng*., 2016. http://dx.doi.org/10.1155/2016/5218738.

Gupta, P.K., *et al.* (2014), "Modelling, verification and investigation of behaviour of circular CFST columns", *Struct. Concrete*, **15**(3), 340-349. DOI: 10.1002/suco.201300045.

Han, L.H., *et al.* (2010), "Tests on inclined, tapered and STS concrete-filled steel tubular (CFST) stub columns", *J. Constr. Steel Res.*, **66**(10), 1186-1195. https://doi.org/10.1016/j.jcsr.2010.03.014.

Han, L.H., *et al*. (2014), "Developments and advanced applications of concrete-filled steel tubular (CFST) structures: Members", *J. Constr. Steel Res.*, **100**, 211-228. https://doi.org/10.1016/j.jcsr.2014.04.016.

Hosseinpour, E., *et al*. (2018), "Direct shear behavior of concrete filled hollow steel tube shear connector for slim-floor steel beams", *Steel Compos. Struct.*, **26**(4), 485-499. https://doi.org/10.12989/scs.2018.26.4.485.

Jalali, A., *et al*. (2012), "Seismic performance of structures with pre-bent strips as a damper", *Int. J. Phys. Sci*., **7**(26), 4061-4072.

Katebi, J., *et al.* (2019), "Developed comparative analysis of metaheuristic optimization algorithms for optimal active control of structures", *Engineering with Computers*, 1-20. https://doi.org/10.1007/s00366-019-00780-7.

Khorami, M., *et al*. (2017a), "Seismic performance evaluation of buckling restrained braced frames (BRBF) using incremental nonlinear dynamic analysis method (IDA)", *Earthq. Struct*., **13**(6), 1-6. http://dx.doi.org/10.12989/eas.2017.13.6.531.

Khorami, M., *et al*. (2017b), "Evaluation of the seismic performance of special moment frames using incremental nonlinear dynamic analysis", *Struct. Eng. Mech*., **63**(2), 259-268. http://dx.doi.org/10.12989/sem.2017.63.2.259.

Khorramian, K., *et al*. (2015), "Behavior of Tilted Angle Shear Connectors", *PLoS One*, **10**(12), e0144288. 10.1371/journal.pone.0144288.

Khorramian, K., *et al*. (2016), "Behavior of tilted angle shear connectors", *PLoS One*, **11**(2). https://doi.org/10.1371/journal.pone.0148945.

Khorramian, K., *et al*. (2017), "Numerical analysis of tilted angle shear connectors in steel-concrete composite systems", *Steel Compos. Struct*., **23**(1), 67-85. http://dx.doi.org/10.12989/scs.2017.23.1.067.

Kildashti, K., *et al*. (2019), "Seismic collapse assessment of a hybrid cold-formed hot-rolled steel building", *J. Constr. Steel Res*., **155**, 504-516. https://doi.org/10.1016/j.jcsr.2019.01.010.

Lee, S., *et al.* (2011),. "Structural characteristics of welded built-up square concrete filled tubular stub columns associated with concrete strength", *Procedia Eng*., **14**, 1140-1148. https://doi.org/10.1016/j.proeng.2011.07.143.

Li, D., *et al.* (2019), "Application of polymer, silica-fume and crushed rubber in the production of Pervious concrete", *Smat Struct. Syst*., **23**(2), 207-214. http://dx.doi.org/10.12989/sss.2019.23.2.207.

Luo, Z., *et al.* (2019), "Computational and experimental analysis of beam to column joints reinforced with CFRP plates", *Steel Compos. Struct.*, **30**(3), 271-280. http://dx.doi.org/10.12989/scs.2019.30.3.271.

Mansouri, I., *et al*. (2019), "Analysis of influential factors for predicting the shear strength of a V-shaped angle shear connector in composite beams using an adaptive neuro-fuzzy technique", *J. Intel. Manufact*., **30**(3), 1-11. https://doi.org/10.1007/s10845-017-1306-6.

Milovancevic, M., *et al.* (2019), "UML diagrams for dynamical monitoring of rail vehicles", *Physica A: Stat. Mech. Appl*., 121169.

Mohammadhassani, M., *et al*. (2014a). "An experimental study on the failure modes of high strength concrete beams with particular references to variation of the tensile reinforcement ratio", *Eng. Fail. Anal*., **41**, 73-80. https://doi.org/10.1016/j.engfailanal.2013.08.014.

Mohammadhassani, M., *et al.* (2014b), "An evolutionary fuzzy modelling approach and comparison of different methods for shear strength prediction of high-strength concrete beams without stirrups", *Smart Struct. Syst.*, **14**(5), 785-809. http://dx.doi.org/10.12989/sss.2014.14.5.785.

Mortazavi, M., *et al*. (2020), "Prefabricated hybrid steel wall panels for mid-rise construction in seismic regions", *J. Build. Eng*., **27**, 100942. https://doi.org/10.1016/j.jobe.2019.100942.

Nasrollahi, S., *et al.* (2018), "Investigation of pipe shear connectors using push out test", *Steel Compos. Struct.*, **27**(5), 537-543. http://dx.doi.org/10.12989/scs.2018.27.5.537.

Paknahad, M., *et al.* (2018), "Shear capacity equation for channel shear connectors in steel-concrete composite beams", *Steel Compos. Struct.*, **28**(4), 483-494. http://dx.doi.org/10.12989/scs.2018.28.4.483.

Petrus, A. and Alfonsi, P. (2006), Dialogue against the Jews, CUA Press.

Saberian, M., *et al.* (2018), "Experimental and phenomenological study of the effects of adding shredded tire chips on geotechnical properties of peat", *Int. J. Geotech. Eng*., **12**(4), 347-356. https://doi.org/10.1080/19386362.2016.1277829.

Sadeghipour Chahnasir, E., *et al.* (2018), "Application of support vector machine with firefly algorithm for investigation of the factors affecting the shear strength of angle shear connectors", *Smart Struct. Syst.*, **22**(4), 413-424. http://dx.doi.org/10.12989/sss.2018.22.4.413.

Safa, M., *et al.* (2016), "Potential of adaptive neuro fuzzy inference system for evaluating the factors affecting steel-concrete composite beam's shear strength", *Steel Compos. Struct.*, **21**(3), 679-688. http://dx.doi.org/10.12989/scs.2016.21.3.679.

Sajedi, F. and Shariati, M. (2019), "Behavior study of NC and HSC RCCs confined by GRP casing and CFRP wrapping", *Steel Compos. Struct.*, **30**(5), 417-432. http://dx.doi.org/10.12989/scs.2019.30.5.417.

Sedghi, Y., *et al.* (2018), "Application of ANFIS technique on performance of C and L shaped angle shear connectors", *Smart Struct. Syst*., **22**(3), 335-340. http://dx.doi.org/10.12989/sss.2018.22.3.335

Shah, S., *et al*. (2015), "Steel rack connections: Identification of most influential factors and a comparison of stiffness design methods", *PLoS One*, **10**(10), e0139422. https://doi.org/10.1371/journal.pone.0139422.

Shah, S., *et al.* (2016a), "Behavior of industrial steel rack connections", *Mech. Syst. Signal Pr*., **70-71**, 725-740. https://doi.org/10.1016/j.ymssp.2015.08.026.

Shah, S., *et al.* (2016b), "Behavior of steel pallet rack beam-to-column connections at elevated temperatures", *Thin-Wall. Struct*., **106**, 471-483. https://doi.org/10.1016/j.tws.2016.05.021.

Shahabi, S., *et al.* (2016a), "Numerical analysis of channel connectors under fire and a comparison of performance with different types of shear connectors subjected to fire", *Steel Compos. Struct.*, **20**(3), 651-669. http://dx.doi.org/10.12989/scs.2016.20.3.651.

Shahabi, S., *et al*. (2016b), "Performance of shear connectors at elevated temperatures-A review", *Steel Compos. Struct.*, **20**(1), 185-203. http://dx.doi.org/10.12989/scs.2016.20.1.185.

Sharafi, P., *et al.* (2018a), "Interlocking system for enhancing the integrity of multi-storey modular buildings", *Automat. Constr*. **85**, 263-272. https://doi.org/10.1016/j.autcon.2017.10.023.

Sharafi, P., *et al.* (2018b), "Lateral force resisting systems in lightweight steel frames: recent research advances", *Thin-Wall. Struct*., **130**, 231-253. https://doi.org/10.1016/j.tws.2018.04.019.

Sharafi, P., *et al.* (2018c), "Identification of factors and decision analysis of the level of modularization in building construction", *J. Architect. Eng*., **24**(2), 04018010. https://doi.org/10.1061/(ASCE)AE.1943-5568.0000313.

Shariat, M., *et al.* (2018), "Computational Lagrangian Multiplier Method by using for optimization and sensitivity analysis of rectangular reinforced concrete beams", *Steel Compos. Struc*t., **29**(2), 243-256. http://dx.doi.org/10.12989/scs.2018.29.2.243.

Shariati, A., *et al.* (2012a), "Investigation of channel shear connectors for composite concrete and steel T-beam", *Int. J. Phys. Sci.*, **7**(11), 1828-1831. DOI: 10.5897/IJPS11.1604.

Shariati, M., *et al*. (2010), "Experimental and analytical study on channel shear connectors in light weight aggregate concrete", *Proceedings of the 4th international conference on steel & composite structures*.

Shariati, M., *et al*. (2011a), "Experimental and numerical investigations of channel shear connectors in high strength concrete", *Proceedings of the 2011 world congress on advances in structural engineering and mechanics (ASEM'11+)*.

Shariati, M., *et al*. (2011b), "Behavior of channel shear connectors in normal and light weight aggregate concrete (experimental and analytical study)", *Adv. Materi.Res*., **168-170**, 2303-2307. https://doi.org/10.4028/www.scientific.net/AMR.168-170.2303.

Shariati, M., *et al.* (2011c), "Shear resistance of channel shear connectors in plain, reinforced and lightweight concrete", *Scientific Res. Essays*, **6**(4), 977-983. DOI: 10.5897/SRE10.1120.

Shariati, M., *et al.* (2012b), "Fatigue energy dissipation and failure analysis of channel shear connector embedded in the lightweight aggregate concrete in composite bridge girders", *Proceedings of the 5th international conference on engineering failure analysis*.

Shariati, M., *et al.* (2012c), "Experimental assessment of channel shear connectors under monotonic and fully reversed cyclic loading in high strength concrete", *Mater. Design*, **34**, 325-331. https://doi.org/10.1016/j.matdes.2011.08.008.

Shariati, M., *et al*. (2013), "Comparison of behaviour between channel and angle shear connectors under monotonic and fully reversed cyclic loading", *Constr. Build. Mater.*, **38**, 582-593. https://doi.org/10.1016/j.conbuildmat.2012.07.050.

Shariati, M., *et al.* (2014), "Fatigue energy dissipation and failure analysis of angle shear connectors embedded in high strength concrete", *Eng. Fail. Anal*., **41**, 124-134. https://doi.org/10.1016/j.engfailanal.2014.02.017.

Shariati, M., *et al.* (2016), "Comparative performance of channel and angle shear connectors in high strength concrete composites: An experimental study", *Constr. Build. Mater*., **120**, 382-392. DOI: 10.1016/j.conbuildmat.2016.05.102.

Shariati, M., *et al.* (2018), "Experimental investigations on monotonic and cyclic behavior of steel pallet rack connections", *Eng. Fail. Anal*., **85**, 149-166. DOI: 10.1016/j.engfailanal.2017.08.014.

Shariati, M., *et al.* (2019a), "Application of waste tire rubber aggregate in porous concrete", *Smart Struct. Syst.*, **24**(4), 553-566. https://doi.org/10.12989/sss.2019.24.4.553.

Shariati, M., *et al.* (2019b), "Application of Extreme Learning Machine (ELM) and Genetic Programming (GP) to design steel-concrete composite floor systems at elevated temperatures", *Steel Compos. Struct.*, **33**(3), 319-332. https://doi.org/10.12989/scs.2019.33.3.319.

Shariati, M., *et al*. (2019c). "Experimental investigation on the effect of cementitious materials on fresh and mechanical properties of self-consolidating concrete", *Adv. Concrete Constr*., **8**(3), 225-237. https://doi.org/10.12989/acc.2019.8.3.225.

Shariati, M., *et al.* (2019d), "Numerical study on the structural performance of corrugated low yield point steel plate shear walls with circular openings", *Steel Compos. Struct.*, **33**(4), 569-581.DOI: https://doi.org/10.12989/scs.2019.33.4.569

Shariati, M., *et al.* (2019e). "Moment-rotation estimation of steel rack connection using extreme learning machine", *Steel Compos. Struct.*, **31**(5), 427-435. http://dx.doi.org/10.12989/scs.2019.31.5.427.

Shariati, M. *et al.* (2019), "Application of a hybrid artificial neural network-particle swarm optimization (ANN-PSO) model in behavior prediction of channel shear connectors embedded in normal and high-strength concrete", *Appl. Sciences*, **9**(24), 55-34. DOI: https://doi.org/10.3390/app9245534.

Shariati, *M*., et al. (2020), "A novel approach to predict shear strength of tilted angle connectors using artificial intelligence techniques", Engineering with Computers. DOI: 10.1007/s00366-019-00930-x.

Sinaei, H., *et al*. (2011), "Numerical investigation on exterior reinforced concrete Beam-Column joint strengthened by composite fiber reinforced polymer (CFRP)", *Int. J. Phys. Sci.*,

6(28), 6572-6579. DOI: 10.5897/IJPS11.1225.
Sinaei, H., *et al.* (2012), "Evaluation of reinforced concrete beam behaviour using finite element analysis by ABAQUS", *Sci. Res. Essays*, **7**(21), 2002-2009. DOI: 10.5897/SRE11.1393.
Suhatril, M., *et al.* (2019), "Significance of surface eco-protection techniques for cohesive soils slope in selangor, Malaysia", *Geotech. Geological Eng*., **37**(3), 2007-2014. https://doi.org/10.1007/s10706-018-0740-3.
Taheri, E., *et al.* (2019), "Investigation of a method for strengthening perforated cold-formed steel profiles under compression loads", *Appl. Sciences*, **9**(23), 5085. https://doi.org/10.3390/app9235085.
Tahmasbi, F., *et al*. (2016), "Shear capacity of C-shaped and L-shaped angle shear connectors", *PLoS One*, **11**(8), e0156989.DOI: 10.1371/journal.pone.0156989.
Tao, Z., *et al*. (2005), "Experimental behaviour of stiffened concrete-filled thin-walled hollow steel structural (HSS) stub columns", *J. Constr. Steel Res*., **61**(7), 962-983. https://doi.org/10.1016/j.jcsr.2004.12.003.
Toghroli, A., *et al*. (2014), "Prediction of shear capacity of channel shear connectors using the ANFIS model", *Steel Compos. Struct*., **17**(5), 623-639. http://dx.doi.org/10.12989/scs.2014.17.5.623.
Toghroli, A. (2015), Applications of the ANFIS and LR models in the prediction of shear connection in composite beams/Ali Toghroli, University of Malaya.
Toghroli, A., *et al.* (2016), "Potential of soft computing approach for evaluating the factors affecting the capacity of steel–concrete composite beam", *J. Intel. Manufact*., 1-9. https://doi.org/10.1007/s10845-016-1217-y.
Toghroli, A., *et al*. (2017), "Investigation on composite polymer and silica fume–rubber aggregate pervious concrete", *Proceedings of the 5th International Conference on Advances in Civil, Structural and Mechanical Engineering - CSM 2017*, Zurich, Switzerland.
Toghroli, A., *et al.* (2018a), "Evaluation of the parameters affecting the Schmidt rebound hammer reading using ANFIS method", *Comput Concret*, **21**(5), 525-530. http://dx.doi.org/10.12989/cac.2018.11.5.525.
Toghroli, A., *et al*. (2018b), "A review on pavement porous concrete using recycled waste materials", *Smart Struct. Syst*., **22**(4), 433-440. http://dx.doi.org/10.12989/sss.2018.22.4.433.
Trung, N.T., *et al*. (2019a), "Reduction of cement consumption by producing smart green concretes with natural zeolites", *Smart Struct. Syst*., **24**(3), 415-425. http://dx.doi.org/10.12989/sss.2019.24.3.415.
Trung, N.T., *et al.* (2019b), "Moment-rotation prediction of precast beam-to-column connections using extreme learning machine", *Struct. Eng. Mech*., **70**(5), 639-647. https://doi.org/10.12989/sem.2019.70.5.639.
Vali, R., *et al*. (2019), "A three-dimensional numerical comparison of bearing capacity and settlement of tapered and under-reamed piles", *Int. J. Geotech. Eng*., **13**(3), 236-248. https://doi.org/10.1080/19386362.2017.1336586.
Wei, X., *et al.* (2018), "Distribution of shear force in perforated shear connectors", *Steel Compos. Struct*., **27**(3), 389-399. http://dx.doi.org/10.12989/scs.2018.27.3.389
Whittle, J. and Ramseyer, C. (2009), "Buckling capacities of axially loaded, cold-formed, built-up C-channels", *Thin-Wall. Struct.*, **47**(2), 190-201. https://doi.org/10.1016/j.tws.2008.05.014.
Xie, Q., *et al.* (2019), "An experimental study on the effect of CFRP on behavior of reinforce concrete beam column connections", *Steel Compos. Struct*., **30**(5), 433-441. http://dx.doi.org/10.12989/scs.2019.30.5.433.
Xu, C., *et al*. (2019), "Using genetic algorithms method for the paramount design of reinforced concrete structures", *Struct. Eng. Mech*., **71**(5), 503-513. https://doi.org/10.12989/sem.2019.71.5.503.
Yan, L. (2016). "Plain concrete cylinders and beams externally strengthened with natural flax fabric reinforced epoxy composites", *Mater. Struct*., **49**(6), 2083-2095. https://doi.org/10.1617/s11527-015-0635-1.
Yan, L., *et al*. (2014), "Flax fibre and its composites–A review", *Compos. Part B: Eng*., **56**, 296-317. https://doi.org/10.1016/j.compositesb.2013.08.014.
Yin, P., *et al*. (2016), "Compressive behavior of concrete confined by CFRP and transverse spiral reinforcement. Part A: experimental study", *Mater. Struct*., **49**(3), 1001-1011. https://doi.org/10.1617/s11527-015-0554-1.
Zandi, Y., *et al*. (2018), "Computational investigation of the comparative analysis of cylindrical barns subjected to earthquake", *Steel Compos. Struct*., **28**(4), 439-447. http://dx.doi.org/10.12989/scs.2018.28.4.439
Zeghiche, J. (2013), "Further tests on thin steel and composite fabricated stubs", *J. Constr. Steel Res*., **81**, 124-137. https://doi.org/10.1016/j.jcsr.2012.11.006.

CC